# Strain in buried quantum wires: Analytical calculations and x-ray diffraction study

V. M. Kaganer, B. Jenichen, G. Paris, and K. H. Ploog
*Paul-Drude-Institut für Festkörperelektronik, Hausvogteiplatz 5-7, D-10117 Berlin, Germany*

O. Konovalov
*European Synchrotron Radiation Facility, BP220, Grenoble, France*

P. Mikulík*
*Fraunhofer Institut für Zerstörungsfreie Prüfverfahren, EADQ, Krügerstr. 22, D-01326 Dresden, Germany*

S. Arai
*Research Center for Quantum Effect Electronics, Tokyo Institute of Technology, 2-12-1 O-okayama, Meguro-ku, Tokyo 152-8552, Japan*

The displacement field in and around periodically arranged quantum wires embedded in a crystalline matrix is calculated analytically for an arbitrary finite thickness of the cover layer. A good agreement is obtained between measured x-ray-diffraction peaks of a wire structure and kinematical calculations with the displacement field derived in the paper. The strain and quantum size effects on the photoluminescence line shift are found to be comparable, due to small width (35 nm) of the wires.

## I. INTRODUCTION

Quantum wires are semiconductor structures which confine electrons in two spatial dimensions. To provide quantum confinement, the cross-sectional sizes of the wires should be comparable with the exciton dimensions, which are typically a few tens of nanometers. Periodic arrays of uniform quantum wires are produced from thin heteroepitaxial layers by means of lithography with subsequent epitaxial overgrowth. An improvement in the performance of semiconductor lasers is expected from the introduction of quantum wire structures into their active region. Quantum wire lasers with a low threshold and a high differential quantum efficiency have been demonstrated.[1]

The difference between lattice spacings of the semiconductor material forming the wire and that of the matrix gives rise to elastic strain. X-ray diffraction is proven to be a very sensitive technique to measure the strain in wires.[2−13] A mean strain in the wires can be obtained simply from positions of the corresponding diffraction peaks or their envelope functions. The strain distribution, however, cannot be directly obtained from the x-ray diffraction pattern, and requires a solution of the elastic equilibrium problem. Up to now x-ray diffraction studies of wire arrays were either restricted with a qualitative analysis and plausible assumptions[2−8] or used laborious finite element calculations.[9−13]

The problem of elastic equilibrium of a periodic array of domains misfitted with respect to the surrounding matrix allows an analytical solution by means of Fourier series expansion. The solutions were obtained for diverse physical applications. The list includes free-standing films with periodic composition modulations studied by transmission electron microscopy,[14−18] free-standing quantum wire multilayers,[19] periodic twinning in a film on a substrate and a thin layer sandwiched within the bulk,[20] and domains of coexisting phases near a structural phase transition in a heteroepitaxial film.[21] None of these solutions can be directly used for an x-ray diffraction study of quantum wires. The cited works present strain, stress,[14−19] or elastic energy,[20] while the displacement field is required to calculate the x-ray diffraction intensity. The displacement field has been calculated in only one study,[21] which, however, does not correspond to the geometry of either free-standing or buried quantum wires. It is also worth mentioning the analytical solution of the elastic problem for a misfitted parallelepiped in a semispace.[22] An infinitely long parallelepiped is identical to an isolated wire but, as we will show below, an assumption of an isolated wire instead of a periodic array of wires introduces a significant error and, again, only stress components were evaluated in Ref. 22.

We obtain analytical expressions for the displacement fields in periodic arrays of buried quantum wires, and apply this solution to an analysis of the x-ray diffraction pattern. We consider periodic arrays of wires with a rectangular cross section. The latter assumption is an appropriate approximation for trapezoidal wires with steep sides commonly obtained by lithography.

We apply x-ray diffractometry to investigate the elastic stress relaxation in $Ga_{0.22}In_{0.78}As_{0.80}P_{0.20}$ quantum wire structures (1% compressively strained) with a wire width of 35 nm and a thickness of 8 nm, similar to the wires in the laser device structures already reported in Ref. 1. We have performed x-ray diffractometric measurements of the strain and measurements of the photoluminescence (PL) line shift on the same samples. We find that the strain and the quantum size effects on the PL line shift are comparable to each other. We note that most of the previous x-ray investigations of wire structures[2−7,10−13] were concerned with wire widths large compared to the quantization dimensions. The smallest wire width still remained as large as 50 nm and the quantum confinement effect was shown to remain small.[3,4]
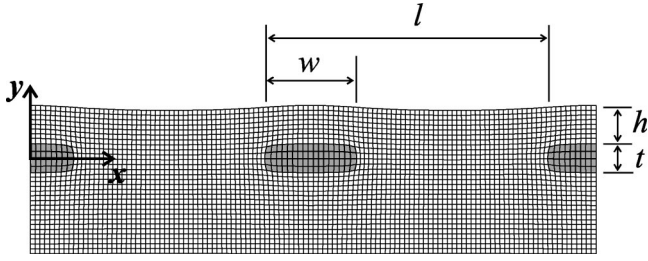
FIG. 1. Geometry of the wires and displacements calculated using the expressions derived in the present paper. Displacements are exaggerated by a factor of 30. Wire width $w=35$ nm, wire height $t=8$ nm, period of the structure $l=120$ nm, thickness of the cover layer $h=20$ nm, and the misfit $\epsilon_0=0.01$.

## II. DISPLACEMENT FIELDS IN AND AROUND THE WIRES

### A. Fourier series expansion

We consider a periodic array of infinitely long crystalline wires coherently embedded into a crystalline matrix, Fig. 1. The cross section of the wires is rectangular, with a width $w$ and a height $t$, and the period of the structure is $l$. The buried wires are covered by the top layer of a finite thickness $h$. The $x$ axis is the direction of periodicity, the $y$ axis is normal to it in the cross-sectional plane, and the $z$ axis is along the wires. The origin is taken to be at the center of the wire. We assume that the wires are infinitely long in the $z$ direction and the substrate is infinitely thick, so that the displacement $u_z$ is identically zero.

The misfit (relative difference between lattice parameters of the two crystalline materials) is assumed to be equal in all three spatial directions, which corresponds to a common case of cubic crystal symmetry of both the wire and the matrix. We solve the elastic problem for a general case of an arbitrary periodic function $\varepsilon(x)$, with the aim of obtaining a solution if a form applicable to other problems involving periodic elastic domains, for example periodic composition modulations.[14–18] The function $\varepsilon(x)$ used to describe the x-ray diffraction pattern in the present paper is equal to a constant $\epsilon_0$ inside the wires ($|x|<w/2$ and $|y|<t/2$, with the periodic repetition along the $x$ axis) and zero outside them.

An even periodic function $\varepsilon(x)$ possessing the period $l$ can be expanded in Fourier series,

$$\varepsilon(x)=\frac{1}{2}\varepsilon_0+\sum_{n=1}^{\infty}\varepsilon_n\cos(2k_nx),\qquad(1)$$

where $k_n=\pi n/l$, and

$$\varepsilon_n=\frac{2}{l}\int_{-l/2}^{l/2}\varepsilon(x)\cos(2k_nx)dx\quad(n=0,1,2,\ldots).\quad(2)$$

In the case of a constant misfit $\epsilon_0$ which will be used to describe the x-ray diffraction pattern, we have

$$\varepsilon_0=2\epsilon_0\frac{w}{l},\quad\varepsilon_n=\frac{2\epsilon_0}{\pi n}\sin(k_nw)\quad(n=1,2,\ldots).\quad(3)$$

The displacement field can also be represented by Fourier series

$$u_x(x,y)=\sum_{n=1}^{\infty}U_n(y)\sin(2k_nx),\qquad(4a)$$

$$u_y(x,y)=V_0(y)+\sum_{n=1}^{\infty}V_n(y)\cos(2k_nx),\qquad(4b)$$

where the functions $U_n(y)$ and $V_n(y)$ are the coefficients in Fourier expansions over $x$. We took into account the reflection symmetry with respect to the $y$ axis and translational invariance along the $z$ axis. The solution of the elastic equilibrium problem is given in the Appendix. The final expressions for the coefficients $U_n(y)$ and $V_n(y)$ are presented in Sec. II B.

### B. Displacements in buried wires

The displacements in buried wires (Fig. 1), can be written separately in the substrate $y<-t/2$,

$$U_n=e_n[\exp(2k_ny)\sinh(k_nt)+R_{xn}],\qquad(5a)$$

$$V_0=0,\qquad(5b)$$

$$V_n=e_n[-\exp(2k_ny)\sinh(k_nt)+R_{yn}];\qquad(5c)$$

in the wire layer $|y|<t/2$ (both inside the wires and between them),

$$U_n=e_n[1-\exp(-k_nt)\cosh(2k_ny)+R_{xn}],\qquad(6a)$$

$$V_0=e_0(y+t/2),\qquad(6b)$$

$$V_n=e_n[\exp(-k_nt)\sinh(2k_ny)+R_{yn}];\qquad(6c)$$

and in the top layer $t/2<y<h+t/2$,

$$U_n=e_n[\exp(-2k_ny)\sinh(k_nt)+R_{xn}],\qquad(7a)$$

$$V_0=e_0t,\qquad(7b)$$

$$V_n=e_n[\exp(-2k_ny)\sinh(k_nt)+R_{yn}].\qquad(7c)$$

Here we denote

$$e_0=\frac{1+\nu}{1-\nu}\varepsilon_0,\quad e_n=\frac{1+\nu}{1-\nu}\frac{\varepsilon_n}{2k_n}\quad(n=1,2,\ldots).\quad(8)$$

$\nu$ is the Poisson ratio, and the finite thickness $h$ of the cover layer gives rise to the terms

$$R_{xn,yn}=[3-4\nu\mp4k_n(y+h-t/2)]$$
$$\times\exp[2k_n(y-t-2h)]\sinh(k_nt),\qquad(9)$$

where the upper sign corresponds to $R_{xn}$ and the lower sign to $R_{yn}$. In the limit of an infinitely thick cover layer, $h\to\infty$, the terms $R_{xn}$ and $R_{yn}$ vanish. The displacements in the limit of a misfitted layer at the surface, $h\to0$, were calculated in Ref. 21.

Figure 1 shows displacements calculated by summation of series (4) with the Fourier components given by Eqs. (5)–(9). The series quickly converges and does not cause any numerical problem.

### C. Strain in buried wires

In the limit of a thick cover layer, $h \to \infty$, the analytical expressions for strain components $u_{xx} = \partial u_x / \partial x, u_{yy} = \partial u_y / \partial y$ can be obtained by summation of the Fourier series for the most important case of a constant misfit, so that Eq. (3) is applicable. First we obtain a notably simple result for the sum $u_{xx} + u_{yy}$. Summation of the series gives

$$u_{xx} + u_{yy} = \frac{1+\nu}{1-\nu} \epsilon_0 \Theta, \qquad (10)$$

where the wire shape function $\Theta(x,y)$ is equal to 1 inside the wire ($|x| < w/2, |y| < t/2$) and 0 outside it.

The expressions for strain can be presented in a compact form by denoting, after Ref. 22, the wire boundaries by $x_i, y_i (i=1,2): x_{1,2} = \mp w/2, y_{1,2} = \mp t/2$. Summation of the series with the use of Eq. (A8) gives, in the wire layer ($|y| < t/2$),

$$u_{xx} = \frac{1+\nu}{1-\nu} \epsilon_0 \left\{ \Theta - \frac{w}{l} + \sum_{i,j=1,2} (-1)^i \right.$$

$$\left. \times \Phi[x - x_i, (-1)^j (y - y_j)] \right\}, \qquad (11)$$

and out of it ($|y| > t/2$),

$$u_{xx} = \frac{1+\nu}{1-\nu} \epsilon_0 \sum_{i,j=1,2} (-1)^{i+j+1} \Phi[x - x_i, -(|y| - y_j)], \qquad (12)$$

where it is denoted

$$\Phi(x,y) = \frac{1}{2\pi} \arctan \frac{e^{2\pi y/l} \sin(2\pi x/l)}{1 - e^{2\pi y/l} \cos(2\pi x/l)}. \qquad (13)$$

In the limit of a large separation between the wires, $t, w \ll l$, the argument of the arctangent in the last equation is $-x/y$ and the stress calculated from Eqs. (10)–(12) reduces to Eqs. (21) and (22) of Ref. 22.

However, the wire width $w$ is usually comparable with the period $l$, while the wire height $t$ is small compared to the period, $t \ll l$. A simple expression for the strain inside the wire can be obtained under this assumption.

$$u_{xx} = \frac{1+\nu}{1-\nu} \frac{\epsilon_0 t}{l} \frac{\sin(\pi w/l)}{\cos(2\pi x/l) - \cos(\pi w/l)} \quad (t \ll l). \quad (14)$$

In this approximation, the strain does not depend on $y$. Equation (14) is valid in all points inside the wire except the vicinity of the boundaries, $|x| = w/2$. In particular, in the wire center ($x=0, y=0$),

$$u_{xx}(0,0) = \frac{1+\nu}{1-\nu} \frac{\epsilon_0 t}{l} \cot \frac{\pi w}{2l} \quad (t \ll l). \qquad (15)$$
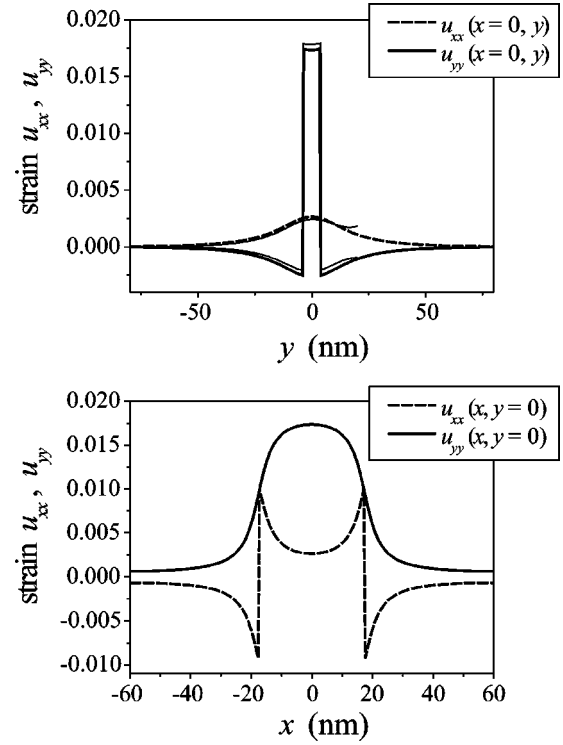


FIG. 2. Strain in the buried wire and around it for an infinite cover layer (thick lines) and a cover layer of thickness $h = 20$ nm (thin lines). All other parameters are the same as in Fig. 1. Vertical and horizontal sections through the wire center are shown in the top and bottom plots, respectively.

If the wire width $w$ is small compared to the period $l$, the latter expression further simplifies to

$$u_{xx}(0,0) = \frac{1+\nu}{1-\nu} \frac{2\epsilon_0 t}{\pi w} \quad (t, w \ll l), \qquad (16)$$

so that the strain depends on the wire aspect ratio $t/w$ only. The strain component $u_{yy}$ can always be obtained from Eq. (10).

Figure 2 shows the strains $u_{xx}$ and $u_{yy}$ in the sections $x=0$ and $y=0$ through the wire center. The sum $u_{xx} + u_{yy}$ satisfies condition (10) at each point $(x,y)$. The strain calculated for a cover layer of thickness $h = 2.5t$ (thin lines) only slightly differs from that calculated for an infinitely thick cover layer (thick lines).

## III. EXPERIMENTAL RESULTS

The wire geometry of the investigated structure is sketched in Fig. 3. The preparation of the samples was described in detail in the earlier works.[8,9] There are no graded layers in the present structures and all the layers except the quantum well (wire) show nearly perfect matching to the InP substrate. In particular, the nominally 100-nm-thick cover layer above the wire gratings shows negligible lattice mismatch. The wires under investigation are sufficiently small to show quantum effects.

High intensity synchrotron radiation is inevitable to detect the diffracted radiation from the strained wires. The x-ray
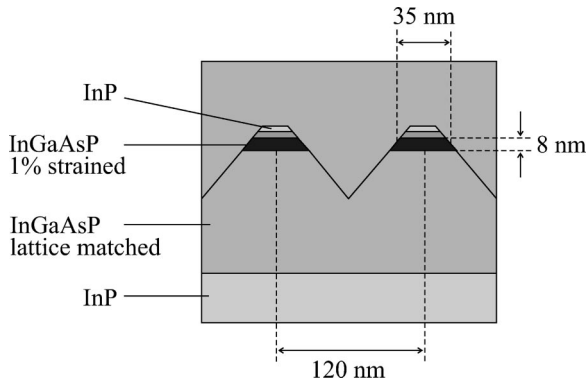
FIG. 3. Schematic view of the quantum wire geometry.

measurements were performed at the European Synchrotron Radiation Facility in Grenoble at the Troïka II undulator beamline (wavelength 0.156 nm, $\Delta\lambda/\lambda = 6\times10^{-5}$). Reciprocal space maps near the (224) reflection (grazing exit) were recorded. Figure 4 demonstrates a map of the wire structure overgrown at 600 °C. The position of the intensity maximum of the wire structure is marked by a cross. The scans through the wire intensity maximum, indicated by arrows in Fig. 4, are shown in Fig. 5 together with the calculated intensity distributions. Calculations were performed by using the kinematic scattering formula

$$I(q_x, q_y) = \left| \int \exp[i\mathbf{Q}\cdot\mathbf{u}(x,y) + i(q_x x + q_y y)]dxdy \right|^2,$$ (17)

where $q_x$ and $q_y$ are the deviations of the scattering vector from the reciprocal-lattice vector $\mathbf{Q}$ and the integration is performed over the half-space occupied by the wire structure and the substrate. The displacement field $\mathbf{u}(x,y)$ is calculated by Eqs. (4) with the coefficents $U_n(y), V_n(y)$ given in Sec. II B.
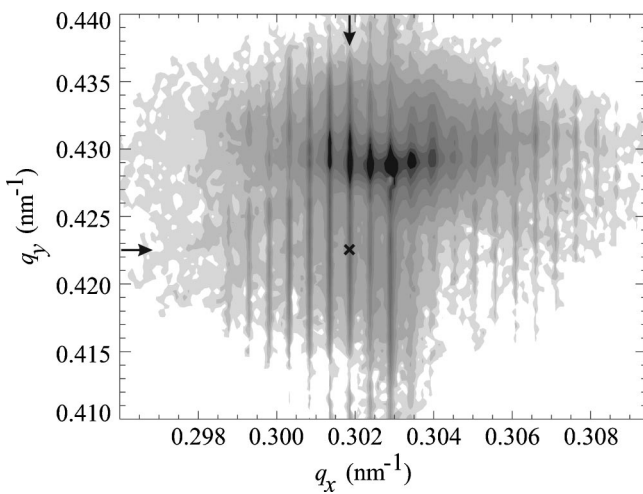


FIG. 4. Reciprocal space map near the asymmetric (224) InP reflection (grazing exit) of the sample with wires buried with nominally 100-nm lattice-matched InGaAsP at a growth temperature of 600 °C. The cross marks the position of the wire intensity maximum.
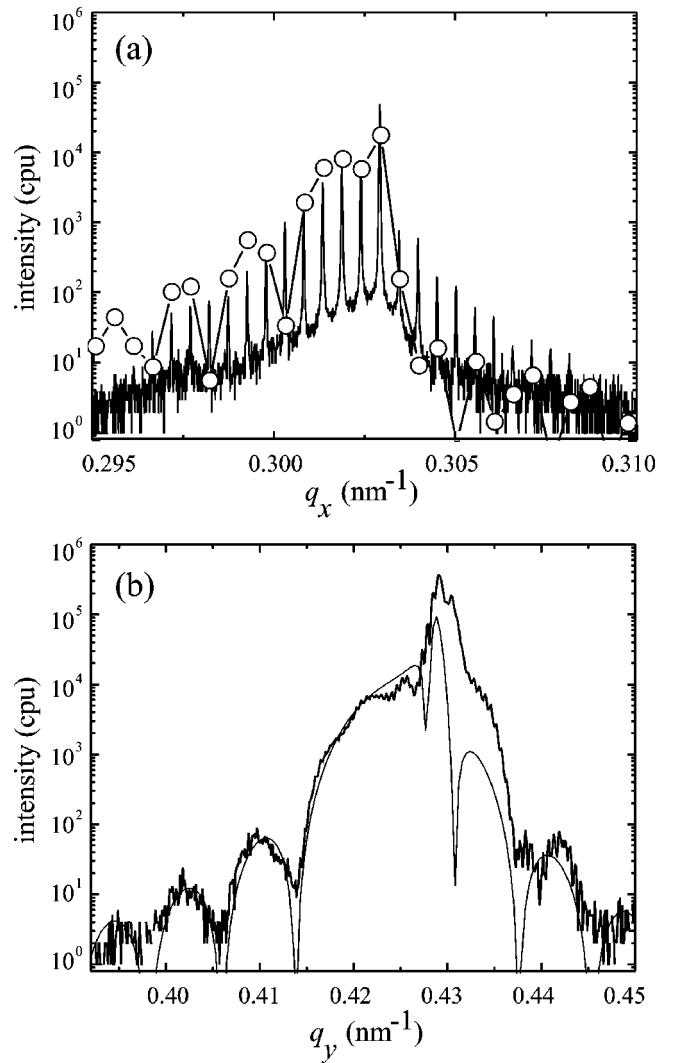


FIG. 5. Intensities in the sections through the wire maximum, indicated by arrows in Fig. 4.

The x-ray diffraction pattern of periodic wires is well understood.[3,4] The long-range periodicity in the wire positions gives rise to narrow (resolution limited) periodic peaks in the $q_x$ direction, Fig. 5(a), with the period $2\pi/l$. The diffuse intensity between the peaks is due to imperfections in wire periodicity.[23] The diffuse intensity is two orders of magnitude lower than the peak intensities, and we do not consider it in the present paper. The peaks are rather broad in the $q_y$ direction [Fig. 5(b)] due to a small thickness $t$ of the wires. The strain in the wires manifests itself in the intensities of the peaks in Fig. 5(a) and in positions of the peaks in Fig. 5(b). Qualitatively, the maximum of an envelope of the satellite peaks is shifted with respect to the substrate peak by $\Delta q_x = -Q_x u_{xx}$ and each satellite is shifted by $\Delta q_y = -Q_y u_{yy}$, where $\mathbf{Q}$ is the diffraction vector. However, the strains $u_{xx}$ and $u_{yy}$ are nonuniform in the wire, and a quantitative determination of the intensities requires a knowledge of the distribution of displacements $u_x(x,y)$ and $u_y(x,y)$. The thin line in Fig. 5(a) is the envelope of the satellite peak intensities calculated in the kinematical theory of x-ray diffraction with the use of the analytical expressions derived

TABLE I. Photoluminescence line shifts $\Delta\lambda$ between patterned and unpatterned regions of the sample. The band-gap change $\Delta E$ and the strain and size contributions are presented.

| Overgrowth temperature ($^\circ$C) | $\Delta\lambda$ (nm) | $\Delta E$ (meV) | $\Delta E_{\text{strain}}$ (meV) | $\Delta E_{\text{size}}$ (meV) |
|---|---|---|---|---|
| 600 | $-33.0$ | 20 | | |
| | | | 8 | 13 |
| 650 | $-37.5$ | 22 | | |

above. The position of the envelope maximum, the decay of the peak intensities, and the asymmetry of the intensity distribution is adequately described. The remaining disagreement in intensities may originate from the trapezoidal cross-sectional shape of the wires (approximated by a rectangle) and some variation in the wire width along the wire, due to an imperfection of the etching. The intensity distribution along the vertical $q_y$ direction through the most intense satellite [Fig. 5(b)] is in a good agreement with the calculations performed with the same displacement field.

Photoluminescence measurements were carried out with an excitation power of 10 mW on a spot of about 100 $\mu$m in diameter at 6 K with a germanium detector using a SPEXS 1681 grating monochromator. The measurements were performed on the patterned and neighboring unpatterned areas in order to detect the quantum wire and quantum-well luminescence near the wavelength of 1450 nm, respectively. In this way, the PL signals of the wires and the neighboring unstructured epitaxial layer stack were compared directly, and the influence of lateral inhomogeneities was kept minimal. A distinct blueshift of the PL lines of the wires with respect to those of the wells was observed. Table I presents the results of the PL measurements performed on two samples, overgrown at 600 and 650 °C.

The additional strain effect on the bandgap of a wire structure with respect to the strained layer (quantum well) is given by the formula[3]

$$\Delta E_{\text{strain}} = a(\Delta u_{xx} + \Delta u_{yy}) + b(\Delta u_{yy} - \Delta u_{xx}/2), \quad (18)$$

where $\Delta u_{xx}$ and $\Delta u_{yy}$ are the differences between corresponding strain components in the wire and in the well. The coefficients $a$ and $b$ are the deformation potentials.[25] We took an interpolation between the values of the endmembers InP, GaAs, InAs, and GaP of the mixed crystal system InGaAsP for the nominal composition of the wires(wells): $a = -6.68$ eV and $b = -1.86$ eV.

The quantum well possesses the strains

$$u_{xx}^{\text{well}} = 0, \quad u_{yy}^{\text{well}} = \frac{1+\nu}{1-\nu}\epsilon_0. \quad (19)$$

We can assume that the recombination takes place only in the central part of the wire, where the energy gap reaches its minimum.[12] Then the strain in the wires can be calculated directly from Eqs. (10) and (15). Using Eq. (10), we find $\Delta u_{xx} + \Delta u_{yy} = 0$, and obtain the relative PL line shift

$$\Delta E_{\text{strain}} = -\tfrac{3}{2} b u_{xx}, \quad (20)$$

where the strain $u_{xx}$ is given by Eq. (15).

The strain effect $\Delta E_{\text{strain}} = 8$ meV thus obtained is less than a half of the band-gap change $\Delta E = 21 \pm 1$ meV. The remaining part of the band-gap change can be attributed to the quantum size effect $\Delta E_{\text{size}} = 13$ meV, which is the difference between the energy of lateral quantization $\Delta E_{\text{lq}}$ and the increase of the exciton binding energy due to lateral confinement $\Delta E_{\text{ex}}$, $\Delta E_{\text{size}} = \Delta E_{\text{lq}} - \Delta E_{\text{ex}}$. We estimate $\Delta E_{\text{ex}} = 2 \pm 1$ meV.[24,25] The shift of the lowest energy level due to lateral quantization in the effective-mass approximation, $\Delta E_{\text{lq}} = \hbar^2 \pi^2 / 2m^* w^2$, gives the effective electron mass $m^* = (0.043 \pm 0.007)m_0$, where $m_0$ is the electron mass. This value has to be compared with the interpolation between those for GaAs, InP, GaP, and InAs crystals,[25,26] which yields $0.06m_0$.

## IV. CONCLUSIONS

We have derived analytical expressions for the displacement field in and around quantum wires of a periodic wire array buried in a crystalline matrix. Particularly simple expressions [Eqs. (10) and (15)] describe strain in the wire center. This result provides a useful tool to estimate the contribution of strain on the photoluminescence line shift. The analytical solution, restricted with the rectangular cross section of the wires and the elastic isotropy, can be used instead of the laborious finite element calculations, if the geometric factors and elastic anisotropy are not of primary importance. We have calculated the x-ray diffraction from the wires using our analytical solution and found a good agreement with the experimental results. We have measured the photoluminescence line shift and found that the contributions of the strain and quantum size effects for the wires under investigation (width 35 nm, height 8 nm) are comparable.

## APPENDIX: SOLUTION OF THE ELASTIC PROBLEM

Our aim is to find the displacement field which is the solution of the elastic equilibrium problem shown in Fig. 1. This displacement field describes a plane strain state with $u_z = 0$, while equal misfits are present in all three spatial directions, $\varepsilon_{pq} = \varepsilon(x)\delta_{pq}$. Here we introduce integer indices $p$ and $q$ running the values 1,2, and 3, and use the coordinates $(x_1, x_2, x_3)$ and $(x, y, z)$ interchangeably. The nonzero misfit $\varepsilon(x)$ in the layer $|y| < t/2$ containing the wires gives rise to the elastic strain $u_{pq} - \varepsilon_{pq}$ and hence to the stress

$\sigma_{pq} = C_{pqp'q'}(u_{p'q'} - \varepsilon_{p'q'})$, where $C_{pqp'q'}$ are the components of the elastic moduli tensor and $u_{pq} = (\partial u_p / \partial x_q + \partial u_q / \partial x_p)/2$. We restrict ourselves with the elastic isotropy, and write the stress as

$$\sigma_{pq} = \frac{E}{1+\nu}\left[ u_{pq} - \varepsilon_{pq} + \frac{\nu}{1-2\nu}(u_{p'p'} - \varepsilon_{p'p'})\delta_{pq} \right], \tag{A1}$$

where $E$ is the Young modulus, $\nu$ is the Poisson ratio, and a summation over repeated indices ($p' = 1,2,3$) is implied. We note that $\varepsilon_{zz} = \varepsilon(x)$, while $u_{zz} = 0$.

The elastic equilibrium equations $\partial \sigma_{pq} / \partial x_q = 0$, expressed through the displacements $u_p$, are

$$(1-2\nu)\left( \frac{\partial^2 u_x}{\partial x^2} + \frac{\partial^2 u_x}{\partial y^2} \right) + \frac{\partial^2 u_x}{\partial x^2} + \frac{\partial^2 u_y}{\partial x \partial y} = 2(1+\nu)\frac{\partial \varepsilon}{\partial x}, \tag{A2a}$$

$$(1-2\nu)\left( \frac{\partial^2 u_y}{\partial x^2} + \frac{\partial^2 u_y}{\partial y^2} \right) + \frac{\partial^2 u_y}{\partial y^2} + \frac{\partial^2 u_x}{\partial x \partial y} = 0. \tag{A2b}$$

The expansion of the displacements $u_x, u_y$ and the misfit $\varepsilon(x)$ in Fourier series [Eqs. (1) and (4)] gives rise to the equations

$$(1-2\nu)U_n'' - 8(1-\nu)k_n^2 U_n - 2k_n V_n' = -4(1+\nu)k_n \varepsilon_n, \tag{A3a}$$

$$(1-\nu)V_n'' - 2(1-2\nu)k_n^2 V_n + k_n U_n' = 0, \tag{A3b}$$

$$V_0'' = 0, \tag{A3c}$$

where the primes denote differentiation over $y$.

The general solution of Eqs. (A3) is

$$U_n = (U_{1n} + U_{2n}y)e^{2k_n y} + (U_{3n} + U_{4n}y)e^{-2k_n y} + \frac{1+\nu}{1-\nu}\frac{\varepsilon_n}{2k_n}, \tag{A4a}$$

$$V_0 = v_1 + v_2 y, \tag{A4b}$$

$$V_n = (V_{1n} + V_{2n}y)e^{2k_n y} + (V_{3n} + V_{4n}y)e^{-2k_n y}, \tag{A4c}$$

where $U_{Mn}, V_{Mn}$ ($M = 1,2,3,4$), and $v_1, v_2$ are constants. Substituting Eq. (A4) into Eq. (A3), one finds

$$V_{1n} = -U_{1n} - \frac{4\nu - 3}{2k_n}U_{2n}, \quad V_{2n} = -U_{2n}, \tag{A5a}$$

$$V_{3n} = +U_{3n} - \frac{4\nu - 3}{2k_n}U_{4n}, \quad V_{4n} = +U_{4n}. \tag{A5b}$$

The solutions of the elastic equilibrium equations in the substrate ($y < -t/2$) and in the cover layer ($y > t/2$) are also given by Eqs. (A4) and (A5), where $\varepsilon_n$ is taken equal to zero and the constants $U_{Mn}$, $V_{Mn}$, $v_1$, and $v_2$ are different in each layer.

These constants can be found by the requirement of absence of tractions at the free boundaries and on the interfaces between the layers ($y = \pm t/2$) and the continuity of the displacements at the interfaces. That is, the requirement that the normal stress $\sigma_{yy}$ is zero at the free surface and continuous on the interfaces reduces to the same requirement for each Fourier component: the quantity

$$(1-\nu)V_n' + 2\nu k_n U_n - (1+\nu)\varepsilon_n \tag{A6}$$

is zero at the free surface and continuous at the interfaces. The last term in Eq. (A6), containing $\varepsilon_n$, is present only in the wire layer ($|y| < t/2$). A similar condition for the shear stress $\sigma_{xy}$ requires zeroing, or a continuity of

$$U_n' - 2k_n V_n. \tag{A7}$$

The continuity of the displacements $u_x$ and $u_y$ at the interfaces is equivalent to continuity of $U_n$ and $V_n$.

The buried wires (Fig. 1) are described by Fourier components of displacements (A4) written separately in the substrate ($y < -t/2$), in the wire layer ($|y| < t/2$), and in the top layer ($t/2 < y < h$). From the 12 unknown coefficients thus introduced, two coefficients describing growing exponents in the substrate are equal to zero, since in the limit $y \to -\infty$ the displacements are absent. The remaining ten coefficients are related by the requirements of the absence of stresses $\sigma_{yy}$ and $\sigma_{xy}$ on the top surface and the continuity of stresses and displacements $\sigma_{yy}, \sigma_{xy}, u_x, u_y$ at two interfaces $y = \pm t/2$. The solution of ten linear equations with ten unknowns is given by Eqs. (5)–(7). The summation of series for the strain components is performed by using the formula[27]

$$\sum_{n=1}^{\infty} \frac{r^n}{n}\sin nx = \arctan\frac{r\sin x}{1 - r\cos x}. \tag{A8}$$

---

*On leave from the Laboratory of Thin Films and Nanostructures, Masaryk University, Kotlářská 2, Brno, Czech Republic.

[1] T. Kojima, M. Tamura, H. Nakaya, S. Tanaka, S. Tamura, and S. Arai, Jpn. J. Appl. Phys. **37**, 261 (1998).

[2] L. Tapfer, G.C. La Rocca, H. Lage, R. Cigolani, P. Grambow, A. Fischer, D. Heitmann, and K. Ploog, Surf. Sci. **267**, 227 (1992).

[3] Q. Shen, S.W. Kycia, E.S. Tentarelli, W.J. Schaff, and L.F. Eastman, Phys. Rev. B **54**, 16 381 (1996).

[4] Q. Shen and S. Kycia, Phys. Rev. B **55**, 15 791 (1997).

[5] L. Leprince, G.T. Baumbach, A. Talneau, M. Gailhanou, and J. Schneck, Appl. Phys. Lett. **71**, 3227 (1997).

[6] G. Baumbach, D. Lübbert, U. Pietsch, N. Darowski, L. Leprince, A. Talneau, and J. Schneck, Physica B **248**, 343 (1998).

[7] N. Darowski, U. Pietsch, Y. Zhuang, S. Zerlauth, G. Bauer, D. Lübbert, and T. Baumbach, Appl. Phys. Lett. **73**, 806 (1998).

[8] B. Jenichen, H.T. Grahn, T. Kojima, and S. Arai, Appl. Phys. **83**, 5810 (1998).

[9] D. Lübbert, B. Jenichen, T. Baumbach, H.T. Grahn, G. Paris, A. Mazuelas, T. Kojima, and S. Arai, J. Phys. D **32**, A21 (1999).

[10] A. Ulyanenkov, T. Baumbach, N. Darowski, U. Pietsch, K.H. Wang, A. Forchel, and T. Wiebach, J. Appl. Phys. **85**, 1524 (1999).

[11] A. Ulyanenkov, N. Darowski, J. Grenzer, U. Pietsch, K.H. Wang, and A. Forchel, Phys. Rev. B **60**, 16 701 (1999).

[12] U. Pietsch, N. Darowski, A. Ulyanenkov, J. Grenzer, K.H. Wang, and A. Forchel, Physica B **283**, 92 (2000).

[13] Y. Zhuang, U. Pietsch, J. Stangl, V. Holý, N. Darowski, J. Grenzer, S. Zerlauth, F. Schäffler, and G. Bauer, Physica B **283**, 130 (2000).

[14] J.M. Gibson and M.M.J. Treacy, Ultramicroscopy **14**, 345 (1984).

[15] M.M.J. Treacy, J.M. Gibson, and A. Howie, Philos. Mag. A **51**, 389 (1985).

[16] M.M.J. Treacy and J.M. Gibson, J. Vac. Sci. Technol. B **4**, 1458 (1986).

[17] D.D. Perovic, G.C. Weatherly, and D.C. Houghton, J. Vac. Sci. Technol. A **6**, 1333 (1988).

[18] D.D. Perovic, G.C. Weatherly, and D.C. Houghton, Philos. Mag. A **64**, 1 (1991).

[19] L. De Caro, L. Tapfer, and A. Giuffrida, Phys. Rev. B **54**, 10 575 (1996).

[20] N. Sridhar, J.M. Rickman, and D.J. Srolovitz, Acta Mater. **44**, 4085 (1996).

[21] V. M. Kaganer, B. Jenichen, F. Schippan, W. Braun, L. Däweritz, and K. H. Ploog, Phys. Rev. B (to be published).

[22] S.M. Hu, J. Appl. Phys. **66**, 2741 (1989).

[23] V. Holý, A.A. Darhuber, G. Bauer, P.D. Wang, Y.P. Song, C.M. Sotomayor Torres, and M.C. Holland, Phys. Rev. B **52**, 8348 (1995).

[24] W. Braun, M. Bayer, A. Forchel, H. Zull, J.P. Reithmaier, A.I. Filin, S.N. Walck, and T.L. Reinecke, Phys. Rev. B **55**, 9290 (1997).

[25] P. Y. Yu and M. Cardona, *Fundamentals of Semiconductors* (Springer, Berlin, 1996).

[26] D. Bimberg *et al.*, in *Semiconductors, Physics of Group IV Elements and III-V Compounds*, edited by O. Madelung, Landolt-Börnstein, New Series, Group III (Springer-Verlag, Berlin, 1982), Vol. 17, Pt. a, p. 144.

[27] A. P. Prudnikov, Y. A. Brychkov, and O. I. Marichev, *Elementary Functions*, Integrals and Series Vol. 1 (Gordon and Breach, New York, 1986).